Suplemento de la Revista Mexicana de Física **3** 020726 (2022) 1–9

Flavourful axion and the Peccei-Quinn symmetry

Stefan Nellen

Insituto de Física, UNAM,
Apartado Postal 20-364, Ciudad de México 01000, México.
Now at Institut für Theoretische Physik, Universität Heidelberg,
Philosophenweg 16, 69120 Heidelberg, Germany.

Received 21 January 2022; accepted 2 June 2022

A model is presented, where the Froggatt-Nielsen and Peccei-Quinn symmetries are identified. This provides a solution to the strong CP problem and an explanation to the fermion mass hierarchy. At leading order, the quark mass matrix possess a Nearest-Neighbour-Interaction structure, while the neutrino mass matrix has a Majorana A_2 texture. From a thorough numerical analysis the viability of this model is asserted, by comparing against current measurements. The data obtained from this analysis is then used to study properties from the axion.

Keywords: Peccei-Quinn; Froggatt-Nielsen; axion; axiflavon; flavourful axion.

DOI: https://doi.org/10.31349/SuplRevMexFis.3.020726

1. Introduction

The Peccei-Quinn (PQ) symmetry, $U(1)_{PQ}$, is a global, axial, abelian symmetry, which was introduced by Peccei and Quinn [1, 2] to provide a solution to the strong CP problem.[i] The idea of this solution is to introduce the PQ symmetry, accompanied by a scalar σ ensuring the symmetry breaks to QCD in such a way that it acts upon the θ-term of QCD, rendering it unphysical. Shortly afterwards, Weinberg [5] and Wilczek [6] independently found that the spontaneous breaking of the PQ symmetry gives rise to a pseudo-Goldstone boson,[ii] which is now called the *axion*.

Another important aspect of the PQ symmetry are its breaking patterns. The effective PQ model rests on a dimension-5 operator, the axion-gluon coupling to remove the θ-term from the QCD lagrangian. Important observables in this theory are the axion mass m_a, the axion-photon coupling $g_{a\gamma}$, and the axion-electron coupling g_{ae} [7]. These can be constrained by experiments. On the other hand, the higher dimension operators can be generated from theories with at most dimension-4 operators, where the assignment of the fermion's PQ charges determines relationships between the axion's observables. The two standard realizations of a UV axion model are the Kim-Shifman-Vainshtein-Zakharov (KSVZ) model [8, 9], where PQ-charged, heavy, vector-like fermions are added, and the Dine-Fischler-Srednicki-Zhitnitsky (DFSZ) model [10, 11], where the Higgs sector is extended with an additional heavy, PQ-charged scalar $SU(2)_L$ doublet.[iii]

In this work, a DFSZ-like model [13] is presented and built, where the PQ symmetry is treated as a flavour symmetry. This model extends both the quark and the lepton sectors. Two UV completions of the quark sector are also considered. Afterwards, properties of the axion are obtained through the branching ratios of flavour violating decays with axions. In Ref. [13], the possibility of flavour changing neutral currents, as well as the axion from this theory being a dark matter candidate, are discussed.

2. The Peccei-Quinn symmetry as a flavour symmetry

The Peccei-Quinn symmetry is well suited to function as a flavour symmetry. Axions from flavour symmetries are usually denominated *flaxions* [14, 15], *axiflavons* [16–18], and *flavourful axions* [19–21].[iv] The most straightforward implementation of the PQ symmetry as a flavour symmetry is by identifying it with the Froggatt-Nielsen (FN) symmetry [22], $U(1)_{FN}$, in other words $U(1)_{PQ} = U(1)_{FN}$. Through careful selection of the PQ-FN (as of now only called PQ) charges, it is possible to incorporate the Froggatt-Nielsen mechanism in KSVZ- and DFSZ-like axion models.

The Froggatt-Nielsen mechanism, similarly to the Peccei-Quinn mechanism, relies on the introduction of a global abelian symmetry, the FN symmetry, and a scalar singlet σ, called the flavon, which carries FN charge, but is otherwise neutral. This singlet couples to the fermions and the Higgs doublet in the following fashion

$$-\mathcal{L}_{FN} \supset y_{ij}^{f^1}\overline{F_L^i}Hf_R^{1\,j}\frac{\sigma^n}{\Lambda^n} + y_{ij}^{f^2}\overline{F_L^i}\widetilde{H}f_R^{2\,j}\frac{\sigma^m}{\Lambda^m}, \quad (1)$$

where F_L^i is the $SU(2)_L$ fermion doublet, while $f_R^{1/2}$ are the right-handed singlets, H the Higgs doublet, $y_{ij}^{f^{1/2}}$ coupling constants, and Λ the FN cut-off scale. The powers n and m are positive integers, whose values are limited by the FN charges of the fermions and the scalars. After the FN symmetry breaks, which should happen before the electroweak (EW) symmetry breaking, these operators become the Standard Model (SM) Yukawa couplings, *i.e.*

$$-\mathcal{L}_Y \supset y_{ij}^{f^1}\overline{F_L^i}Hf_R^{1\,j}\epsilon^n + y_{ij}^{f^2}\overline{F_L^i}\widetilde{H}f_R^{2\,j}\epsilon^m + \mathcal{O}(\Lambda^{-1}). \quad (2)$$

TABLE I. Field content and transformation properties of the PQ-symmetry under the DFSZ type-I seesaw model, where $i = 1, 2, 3$ represents families of three quarks. The PQ charges of the quarks are given in the order of the families' masses, with the lightest as the first.

Fields/Symmetry	Q_{iL}	u_{iR}	d_{iR}	H_u	H_d	σ
$SU(2)_L \times U(1)_Y$	(2, 1/6)	(1, 2/3)	(1, -1/3)	(2, -1/2)	(2, 1/2)	(1, 0)
$U(1)_{PQ}$	(9/2, -5/2, 1/2)	(-9/2, 5/2, -1/2)	(-9/2, 5/2, -1/2)	1	1	1

Here $\epsilon = v_\sigma/\Lambda$, where v_σ is the flavon's vacuum expectation value (*vev*). The SM Yukawa couplings are then $Y_{ij}^{f^{1/2}} = \epsilon^{n/m} y_{ij}^{f^{1/2}}$. If ϵ is small enough, it is possible that the couplings $y_{ij}^{f^{1/2}}$ are all of order $\mathcal{O}(1)$, and the difference in the orders of magnitude in the SM Yukawa couplings comes from differing powers of ϵ. This provides a simple solution to the fermion mass hierarchy problem. For historical reasons, it is common to set $\epsilon \sim \theta_C \approx 0.2$ [23], where θ_C is the Cabibbo angle.

3. A flavourful axion model

The following model consists of a KSVZ-like model. This means that, besides the flavon σ, another Higgs doublet $H_{u/d}$, will be introduced. For consistency in the lepton sector, it will also be necessary to introduce a second flavon σ'. After breaking of the PQ symmetry, it is also possible to extract the axion from the theory's scalars, though its exact composition depends on the UV-completion of the quark sector. Two different UV-completions of the quark sector are provided.

3.1. The quark sector

The PQ-charge assignment for the quarks follows from the standard KSVZ charges for the scalars (see [12]). This assignment ensures that no other abelian symmetries are permitted besides $U(1)_Y$ and $U(1)_{PQ}$, where all the other constraints are set by requiring the operators to be invariant under the PQ and SM symmetries. The PQ charges for the quarks follow from imposing a texture on the quark mass matrices, which in this case is the Nearest-Neighbour-Interaction texture (NNI) [24]. This texture is similar to the Fritzsch texture [25, 26], it has the same zeros, but unlike the Fritzsch texture, it is not necessarily hermitic.[v] The non-zero elements are in the $i = j + 1$, and the $i = N = j$ entries, leading to

$$M^{u/d} = \begin{pmatrix} 0 & \times & 0 \\ \times & 0 & \times \\ 0 & \times & \times \end{pmatrix}. \tag{3}$$

This constraint is not enough to fix the charges, as such, the next constraint is that the $(3, 3)$ entry of the both quark mass matrices is generated at dimension-4, while all the others are generated at dimension-5. The charges and representations of the quarks and scalars can be read off of Table I.

The lagrangian for the up-sector, up to dimension-12, is

$$\begin{aligned} -\mathcal{L} \supset\ & \frac{C^u_{11}}{\Lambda^8}\overline{Q}_{1L} H_u u_{1R} \sigma^8 + \frac{C^u_{12}}{\Lambda}\overline{Q}_{1L} H_u u_{2R} \sigma + \frac{C^u_{13}}{\Lambda^4}\overline{Q}_{1L} H_u u_{3R} \sigma^4 + \frac{C^u_{21}}{\Lambda}\overline{Q}_{2L} H_u u_{1R} \sigma + \frac{C^u_{22}}{\Lambda^4}\overline{Q}_{2L} \widetilde{H}_d u_{2R} \sigma^{*4} \\ & + \frac{C^u_{23}}{\Lambda}\overline{Q}_{2L} \widetilde{H}_d u_{3R} \sigma^* + \frac{C^u_{31}}{\Lambda^4}\overline{Q}_{3L} H_u u_{1R} \sigma^4 + \frac{C^u_{32}}{\Lambda}\overline{Q}_{3L} \widetilde{H}_d u_{2R} \sigma^* + y^u_{33}\overline{Q}_{3L} H_u u_{3R}\,. \end{aligned} \tag{4}$$

Analogously, the down-sector lagrangian reads

$$\begin{aligned} -\mathcal{L} \supset\ & \frac{C^d_{11}}{\Lambda^8}\overline{Q}_{1L} H_d d_{1R} \sigma^8 + \frac{C^d_{12}}{\Lambda}\overline{Q}_{1L} H_d d_{2R} \sigma + \frac{C^d_{13}}{\Lambda^4}\overline{Q}_{1L} H_d d_{3R} \sigma^4 + \frac{C^d_{21}}{\Lambda}\overline{Q}_{2L} H_d d_{1R} \sigma \\ & + \frac{C^d_{22}}{\Lambda^4}\overline{Q}_{2L} \widetilde{H}_u d_{2R} \sigma^{*4} + \frac{C^d_{23}}{\Lambda}\overline{Q}_{2L} \widetilde{H}_u d_{3R} \sigma^* + \frac{C^d_{31}}{\Lambda^4}\overline{Q}_{3L} H_d d_{1R} \sigma^4 + \frac{C^d_{32}}{\Lambda}\overline{Q}_{3L} \widetilde{H}_u d_{2R} \sigma^* + y^d_{33}\overline{Q}_{3L} H_d d_{3R}\,, \end{aligned} \tag{5}$$

where $C_{ij}^{u/d}$ represents the coupling constant of each term and Λ is the FN cut-off scale of the model. After PQ and EW breaking, we get from the FN mechanism, up to dimension-7, the following mass matrices

$$M^{u/d} = \begin{pmatrix} 0 & \varepsilon v_{u/d} C^{u/d}_{12} & 0 \\ \varepsilon v_{u/d} C^{u/d}_{21} & 0 & \varepsilon v_{d/u} C^{u/d}_{23} \\ 0 & \varepsilon v_{d/u} C^{u/d}_{32} & y^{u/d}_{33} v_{u/d} \end{pmatrix}, \tag{6}$$

TABLE II. Vector like fermions and their transformation properties of the PQ-symmetry under the DFSZ type-I seesaw model, where $C = L, R$.

Fields/Symmetry	F_{uC}^{12}	F_{uC}^{21}	F_{uC}^{23}	F_{uC}^{32}	F_{dC}^{12}	F_{dC}^{21}	F_{dC}^{23}	F_{dC}^{32}
$U(1)_Y$	2/3	2/3	2/3	2/3	-1/3	-1/3	-1/3	-1/3
$U(1)_{PQ}$	7/2	-7/2	-3/2	3/2	7/2	-7/2	-3/2	3/2

where $\varepsilon = v_\sigma/\Lambda = \langle\sigma\rangle^*/\Lambda$, and $v_{u/d}$ is the *vev* of the up- or down-sector Higgs doublet. Supposing $\varepsilon \sim 0.2$, we can safely neglect contributions from higher dimensions, as these will enter at ε^4. Therefore, we obtain the desired NNI structure for the quark masses. Unlike other FN models, the mass hierarchy between the up- and down-sector is not generated by the ε powers. This is especially noticeable between m_t and m_b. Nevertheless, it can be explained by a hierarchy between v_u and v_d.

3.1.1. UV-completion: Type-I Seesaw

Here, heavy vector-like fermions, F_q^{ij}, which carry colour charge are introduced. These also carry PQ charge and weak hypercharge. Analogously to the type-I seesaw mechanism for neutrinos [29], the fermions are $SU(2)_L$ singlets. Table II contains the charges of the new fermions, while Fig. 1 shows the Feynman diagram corresponding to the UV-completion. The UV-complete Lagrangian for the up-sector, which corresponds to Eq. (4), is

$$\begin{aligned}-\mathcal{L}_u^{UV} \supset\ & \mathcal{Y}_{12}^u \overline{Q}_{1L} H_u F_{uR}^{12} + \mathcal{M}_{12}^u \overline{F_{uR}^{12}} F_{uL}^{12} + \mathcal{Y}'^u_{12}\ \overline{F_{uL}^{12}} \sigma u_{2R} + \mathcal{Y}_{21}^u \overline{Q}_{2L} H_u F_{uR}^{21} + \mathcal{M}_{21}^u \overline{F_{uR}^{21}} F_{uL}^{21} + \mathcal{Y}'^u_{21} \overline{F_{uL}^{21}} \sigma u_{1R} \\ & + \mathcal{Y}_{23}^u \overline{Q}_{2L} \widetilde{H}_d F_{uR}^{23} + \mathcal{M}_{23}^u \overline{F_{uR}^{23}} F_{uL}^{23} + \mathcal{Y}'^u_{23}\ \overline{F_{uL}^{23}} \sigma^* u_{3R} + \mathcal{Y}_{32}^u \overline{Q}_{3L} \widetilde{H}_d F_{uR}^{32} + \mathcal{M}_{32}^u \overline{F_{uR}^{32}} F_{uL}^{32} + \mathcal{Y}'^u_{32} \overline{F_{uL}^{32}} \sigma^* u_{2R}. \end{aligned} \quad (7)$$

Similarly, for the down-sector of Eq. (5) we have

$$\begin{aligned}-\mathcal{L}_d^{UV} \supset\ & \mathcal{Y}_{12}^d \overline{Q}_{1L} H_d F_{dR}^{12} + \mathcal{M}_{12}^d \overline{F_{dR}^{12}} F_{dL}^{12} + \mathcal{Y}'^d_{12}\ \overline{F_{dL}^{12}} \sigma d_{2R} + \mathcal{Y}_{21}^d \overline{Q}_{2L} H_d F_{dR}^{21} + \mathcal{M}_{21}^d \overline{F_{dR}^{21}} F_{dL}^{21} + \mathcal{Y}'^d_{21} \overline{F_{dL}^{21}} \sigma d_{1R} \\ & + \mathcal{Y}_{23}^d \overline{Q}_{2L} \widetilde{H}_u F_{dR}^{23} + \mathcal{M}_{23}^d \overline{F_{dR}^{23}} F_{dL}^{23} + \mathcal{Y}'^d_{23}\ \overline{F_{dL}^{23}} \sigma^* d_{3R} + \mathcal{Y}_{32}^d \overline{Q}_{3L} \widetilde{H}_u F_{dR}^{32} + \mathcal{M}_{32}^d \overline{F_{dR}^{32}} F_{dL}^{32} + \mathcal{Y}'^d_{32} \overline{F_{dL}^{32}} \sigma^* d_{2R}\ . \end{aligned} \quad (8)$$

The heavy fermions, F_q^{ij}, will couple to the left-handed quarks and the Higgs doublets with a Yukawa coupling $\mathcal{Y}_{ij}^q$, and to the flavon and the right-handed quarks with a different Yukawa coupling, $\mathcal{Y}'^q_{ij}$. They mix through the mass terms with $\mathcal{M}_{ij}^q$.

$$m^{u/d} \approx M_{Q_L q_R} - M_{Q_L F_R} M_{F_L F_R}^{-1} M_{F_L q_R}\ . \quad (9)$$

Assuming the new fermions are much more massive than the SM quarks, *i.e.* $M_{F_L q_R} \gg M_{Q_L q_R}, M_{Q_L F_R}, M_{F_L q_R}$, where $M_{\Psi_L \psi_R}$ are the matrices of the quadratic fermion couplings, it is possible to find a relationship for the quark mass matrices, which reads

$$m^{u/d} \approx M_{Q_L q_R} - M_{Q_L F_R} M_{F_L F_R}^{-1} M_{F_L q_R}\ . \quad (10)$$

This is analogous to the type-I seesaw mechanism for neutrinos, where the heavy right-handed neutrinos decouple in the same fashion, with the addition here of an extra term coming from the quark Dirac mass matrix $M_{Q_L q_R}$. For a review on the minimal seesaw mechanisms see [30]. Explicitly these matrices are,

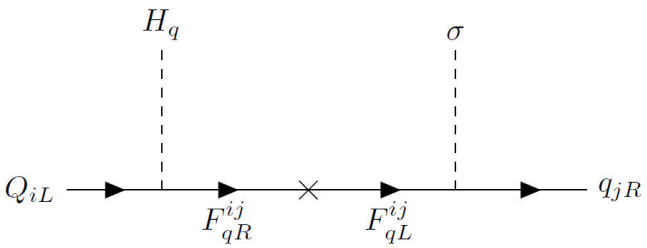

FIGURE 1. UV-complete diagram for the type-I seesaw lagrangian from Eqs. (7) and (8).

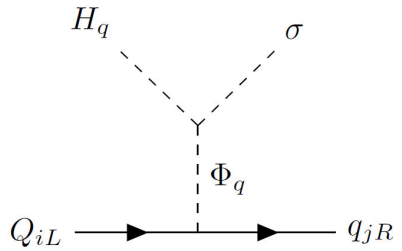

FIGURE 2. UV-complete diagram for the type-II seesaw lagrangian from Eqs. (12) and (13).

$$m^{u/d} = \begin{pmatrix} 0 & \frac{\mathcal{Y}^{u/d}_{12}\mathcal{Y}'^{u/d}_{12}}{\mathcal{M}_{12}} v_{u/d} v_\sigma & 0 \\ \frac{\mathcal{Y}^{u/d}_{21}\mathcal{Y}'^{u/d}_{21}}{\mathcal{M}_{21}} v_{u/d} v_\sigma & 0 & \frac{\mathcal{Y}^{u/d}_{23}\mathcal{Y}'^{u/d}_{23}}{\mathcal{M}_{23}} v^*_{d/u} v^*_\sigma \\ 0 & \frac{\mathcal{Y}^{u/d}_{32}\mathcal{Y}'^{u/d}_{32}}{\mathcal{M}_{32}} v^*_{d/u} v^*_\sigma & y^{u/d}_{33} v_{u/d} \end{pmatrix} , \tag{11}$$

which have the desired NNI texture. It is also worth noting that the suppressing role played by $1/\Lambda$ in the low-energy theory is now taken over by $1/\mathcal{M}_{ij}$, setting a natural scale for these masses at $\mathcal{M}_{ij} \sim \Lambda$.

3.1.2. UV-completion: Type-II Seesaw

For the second UV-completion we introduce two heavy $SU(2)_L$ doublets, $\Phi_{u/d}$. These transform under $SU(2)_L \times U(1)_Y \times U(1)_{PQ}$ in the following representations: Φ_u in $(2,\, -1/2,\, 2)$ representation, and Φ_d in the $(2,\, 1/2,\, 2)$ representation. The topology of the UV-complete diagram, which can be seen in Fig. 2, is the same as type-II seesaw in the neutrino sector [30], hence this UV-completion will be denoted as *type-II seesaw*. The lagrangian of the up-sector (Eq. (4)) is UV-completed as

$$-\mathcal{L}^{UV}_u \supset \mathcal{Y}^u_{12}\overline{Q}_{1L}\Phi_u u_{2R} + \mathcal{Y}^u_{21}\overline{Q}_{2L}\Phi_u u_{1R} + \kappa_u H_u \Phi^\dagger_u \sigma + \mathcal{Y}^u_{23}\overline{Q}_{2L}\widetilde{\Phi}_d u_{3R} + \mathcal{Y}^u_{32}\overline{Q}_{3L}\widetilde{\Phi}_d u_{2R} + \kappa_d \widetilde{H}_d \Phi_d \sigma^* \, . \tag{12}$$

In the same vein, the lagrangian of Eq. (5) becomes

$$-\mathcal{L}^{UV}_d \supset \mathcal{Y}^d_{12}\overline{Q}_{1L}\Phi_d d_{2R} + \mathcal{Y}^d_{21}\overline{Q}_{2L}\Phi_d d_{1R} + \kappa_u H_d \Phi^\dagger_d \sigma + \mathcal{Y}^d_{23}\overline{Q}_{2L}\widetilde{\Phi}_d d_{3R} + \mathcal{Y}^d_{32}\overline{Q}_{3L}\widetilde{\Phi}_d d_{2R} + \kappa_d \widetilde{H}_u \Phi_d \sigma^* \, . \tag{13}$$

In this case, under the assumption that the new scalars are by far the heaviest particles, the mass matrices for the up- and down-quarks read

$$m^{u/d} = \begin{pmatrix} 0 & \mathcal{Y}^{u/d}_{12} v_{\Phi_{u/d}} & 0 \\ \mathcal{Y}^{u/d}_{21} v_{\Phi_{u/d}} & 0 & \mathcal{Y}^{u/d}_{23} v_{\Phi_{d/u}} \\ 0 & \mathcal{Y}^{u/d}_{32} v_{\Phi_{d/u}} & y^{u/d}_{33} v_{u/d} \end{pmatrix} , \tag{14}$$

here the $v_{\Phi_{u/d}}$ are the *vevs* of the heavy doublets, which at leading order are $v_{\Phi_{u/d}} \approx -[\kappa_{u/d} v_\sigma v_{u/d} / M^2_{\Phi_{u/d}}]$, with $M_{\Phi_{u/d}}$ as the masses of $\Phi_{u/d}$. Again, these matrices are of the NNI type. Unlike the type-I seesaw, the correspondence we have now to the FN-cutoff is quadratic in the masses of the new scalars, and inversely proportional to the trilinear coupling, *i.e.* $\Lambda \sim M^2_{\Phi_{u/d}}/\kappa_{u/d}$.

3.2. The Lepton Sector

In the lepton sector a new flavon, σ', is introduced. Alongside it, heavy, right-handed neutrinos are introduced. These couple to the left-handed SM neutrinos, in a such a way that the standard, minimal, type-I seesaw mechanism is realized, as such, this sector is already UV-complete. This is a model building choice made a priori, so that the neutrino mass matrices have the A_2 [31] texture. The representations of the new fields can be read from Table III.

The leptons' Yukawa lagrangian is given by

$$\begin{aligned} -\mathcal{L}^l_y \supset\; & y_e \overline{L}_{eL} H_d \ell_{eR} + y_\mu \overline{L}_{\mu L} \widetilde{H}_u \ell_{\mu R} + y_\tau \overline{L}_{\tau L} H_d \ell_{\tau R} + y^\nu_1 \overline{L}_{eL} H_u N_1 + y^\nu_2 \overline{L}_{\mu L} \widetilde{H}_d N_2 \\ & + y^\nu_3 \overline{L}_\tau H_u N_3 + \frac{M_1}{2} \overline{N^c_1} N_1 + \frac{y^N_{12}}{2} \overline{N^c_1} N_2 \sigma' + \frac{y^N_{13}}{2} \overline{N^c_1} N_3 \sigma + \frac{y^N_{33}}{2} \overline{N^c_3} N_3 \sigma' . \end{aligned} \tag{15}$$

From here it can be seen that the charged lepton mass matrix and the neutrino Dirac mass matrix will be diagonal, whereas the right-handed Majorana mass matrix will not. The inclusions of σ' is required because the $(1,\, 2)$ term for σ is prohibited by the PQ symmetry, as can be seen from Table I and III, and thus the Majorana mass matrix would be singular at leading order in a theory with only the σ flavon.

TABLE III. Field content and transformation properties of the leptons and the flavon σ', where $i = 1, 2, 3$ represent the three lepton families.

Fields/Symmetry	L_{iL}	ℓ_{iR}	N_i	σ'
$SU(2)_L \times U(1)_Y$	(2, -1/2)	(1, -1)	(1, 0)	(1, 0)
$U(1)_{PQ}$	(1, -3, 0)	(0, -2, -1)	(0, -2, -1)	2

The condition for the seesaw mechanism to work, namely that the right-handed neutrinos are much heavier than the left-handed neutrinos, is naturally satisfied, since the PQ symmetry breaks much before the EW symmetry does (only the right-handed neutrinos couple to the flavons). Parametrizing the neutrino mass matrices we have

$$M_R = \begin{pmatrix} M_1 & y_{12}^N v_{\sigma'} & y_{13}^N v_\sigma \\ y_{12}^N v_{\sigma'} & 0 & 0 \\ y_{13}^N v_\sigma & 0 & y_{33}^N v_{\sigma'} \end{pmatrix} \tag{16}$$

and

$$M_D = \mathrm{diag}\left(v_u y_1^\nu,\, v_u^* y_2^\nu, v_d y_3^\nu\right). \tag{17}$$

For the masses of the SM neutrinos we have

$$m_\nu = -M_D^T M_R^{-1} M_D, \tag{18}$$

from the seesaw mechanism. Explicitly, this is

$$m_\nu = \frac{1}{v_{\sigma'}} \begin{pmatrix} 0 & -\frac{v_u v_d^* y_1^\nu y_2^\nu}{y_{12}^N} & 0 \\ -\frac{v_u v_d^* y_1^\nu y_2^\nu}{y_{12}^N} & \frac{(v_d^* y_2^\nu)^2 (M_1 v_{\sigma'} y_{33}^N - v_\sigma^2 (y_{13}^N)^2)}{v_{\sigma'}^2 y_{33}^N (y_{12}^N)^2} & \frac{v_u v_d^* v_\sigma y_2^\nu y_3^\nu y_{13}^N}{v_{\sigma'} y_{12}^N y_{33}^N} \\ 0 & \frac{v_u v_d^* v_\sigma y_2^\nu y_3^\nu y_{13}^N}{v_{\sigma'} y_{12}^N y_{33}^N} & -\frac{v_u^2 (y_3^\nu)^2}{y_{33}^N} \end{pmatrix} \tag{19}$$

and corresponds to the A_2 texture. Much like the quark-sector, the PQ charges of the leptons are chosen in such a way that this texture is obtained.

3.3. The scalar sector

The scalar sector depends on the UV-completion of the quark sector. The full scalar potential is, in both cases, but particularly for the type-II seesaw, rather complicated (see [13]). It has to have specific Higgs-flavon couplings to ensure that the only abelian symmetry in the scalar sector is $U(1)_Y \times U(1)_{PQ}$ [11, 32]. These are $\widetilde{H}_u H_d \sigma'$ and $\widetilde{H}_u H_d \sigma^2$.

To extract the axion from the theory's spectrum it is useful to write down the scalars explicitly. As a matter of fact, the scalars in both UV-completions can be written as

$$\begin{aligned} H_u &= \begin{pmatrix} h_u^0 + iA_u \\ h_u^- \end{pmatrix}, \quad H_d = \begin{pmatrix} h_d^+ \\ h_d^0 + iA_d \end{pmatrix}, \\ \sigma &= S + iA, \quad \sigma' = S' + iA', \\ \Phi_u &= \begin{pmatrix} \phi_u^0 + iA_u' \\ \phi_u^- \end{pmatrix}, \quad \Phi_d = \begin{pmatrix} \phi_d^+ \\ \phi_d^0 + iA_d' \end{pmatrix}, \end{aligned} \tag{20}$$

where $\Phi_{u/d}$ appear only in the second UV-completion of the quark sector. The axion is the PQ Goldstone boson orthogonal to the Goldstone absorbed by the Z, as such it can be expressed as a linear combination of the Goldstone bosons A_i, *i.e.*

$$a = A_{PQ} - \left[\frac{\sum_i X_i Y_i v_i^2}{\sqrt{\sum_i Y_i^2 v_i^2}\sqrt{\sum_i X_i^2 v_i^2}}\right] A_Z\,. \tag{21}$$

Here Y_i is the hypercharge, X_i the PQ-charge, and v_i its *vev* of each scalar field. The other two Goldstone bosons are

$$A_Z = \frac{\sum_i Y_i v_i A_i}{\sqrt{\sum_i Y_i^2 v_i^2}}\,, \tag{22}$$

and

$$A_{PQ} = \frac{\sum_i X_i v_i A_i}{\sqrt{\sum_i X_i^2 v_i^2}}\,. \tag{23}$$

Some properties of this axion can be obtained at this point. The first properties can be inferred from constraints on the *vevs*. It is necessary to replicate SM Higgs *vev*, *i.e.* $\sqrt{\sum_i Y_i^2 v_i^2} \approx 246\,\mathrm{Gev}$. The next constraint is that $\sqrt{\sum_i X_i^2 v_i^2}$ is bounded from below by the value of f_a, the axion decay constant, which is usually a free parameter. For these two constraints to be simultaneously satisfied a strong hierarchy must exist between the *vevs* of the flavons and the Higgs doublets, wherein $v_{\sigma/\sigma'} \gg v_{u/d}$. Furthermore, to avoid mixing between A and A', the condition $v_\sigma \gg v_{\sigma'}$ is imposed. This also generates the mass hierarchy between the quarks and leptons, and implies that the quarks will couple more strongly to the axion than the leptons. The axion decay constant is related to the PQ *vev* as $f_a = v_a/\sqrt{2}N$, where N is the theory's colour anomaly factor [7]. The PQ *vev* is related to the *vevs* of the scalar fields by $v_a = \sqrt{\sum X_i^2 v_i^2}$, which by applying the aforementioned hierarchies reduces the decay constant to

$$f_a \approx \frac{v_\sigma}{\sqrt{2}N}. \tag{24}$$

The mass is inversely proportional to the decay constant [33]

$$m_a \approx 5.70 \left(\frac{10^{12}\,\mathrm{GeV}}{f_a}\right) \mu\mathrm{eV}, \tag{25}$$

and another important observable is the axion-photon coupling $g_{a\gamma}$, which depends on the decay constant and the ratio of the electromagnetic and colour anomaly factors, E/N, as

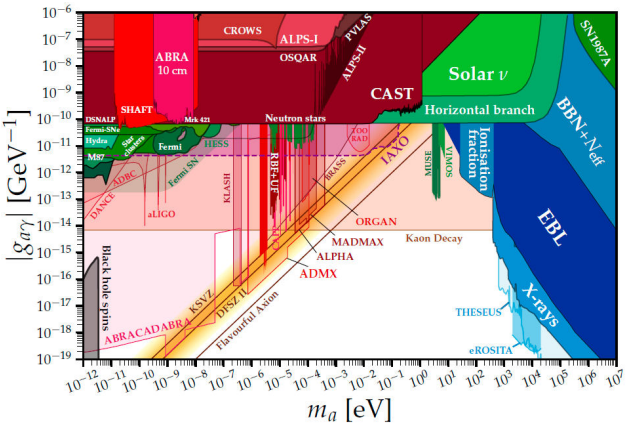

FIGURE 3. Different axion models, including this flavourful axion, and bounds in the $g_{a\gamma} - m_a$ plane. Current bounds are solid, while future projections are transparent. This plot was adapted from [35].

$$g_{a\gamma} = \frac{\alpha}{2\pi f_a}\left(\frac{E}{N} - \frac{2}{3}\frac{m_u + 4m_d}{m_u + m_d}\right) \approx \frac{\alpha}{2\pi f_a}\left(\frac{E}{N} - 1.92\right). \tag{26}$$

In this model $E/N = 28/15 \approx 1.87$, which implies $g_{a\gamma}$ will be small and negative. Compared to a benchmark DFSZ axion, coming from a $SU(5)$ Grand Unified Theory [34], where $E/N = 8/3$, the following relationship is found

$$\frac{|g_{a\gamma}^{SU(5)}|}{|g_{a\gamma}^{Flaxion}|} \approx 14\,, \tag{27}$$

implying this axion is very weakly coupled to the photon. Further constraints on the relationship between mass and the axion-photon coupling can be seen in Fig. 3. Note that the constraint coming from kaon decays applies only to the axion from this model.

4. Numerical Results

4.1. Masses and Mixing Parameters of Fermions

A χ^2 fit is conducted to find the parameters of the mass matrices, which are compared against experiments and global fits. The χ^2 function is defined as follows

$$\chi^2 = \sum \frac{(\mu_{\rm exp} - \mu_{\rm fit})^2}{\sigma_{\rm exp}^2}\,, \tag{28}$$

where the sum runs over all observables. In this equation $\mu_{\rm fit}$ represent the masses and mixing parameters calculated from the mass matrices, while $\mu_{\rm exp}$ and $\sigma_{\rm exp}$ are the observables to be fitted and their standard deviations. The fit is conducted at the M_Z scale [36, 37]. The observable and fitting parameters

TABLE IV. Best-fit values of the model parameters in the quark sector are shown in the upper table. The global best-fit as well as their 1σ error [36, 37] for the various observables are given in the second and third columns of the lower table. Also, the best-fit values of the various observables are listed in the last column of the lower table.

Parameter	Best fit
$A_u/(10^{-2}\,\text{GeV})$	1.493
$B_u/(10^{-2}\,\text{GeV})$	−5.531
$C_u/\,\text{GeV}$	−3.008
$D_u/(10^{1}\,\text{GeV})$	3.562
$E_u/(10^{2}\,\text{GeV})$	1.679
$A_d/(10^{-2}\,\text{GeV})$	−1.241
$B_d/(10^{-2}\,\text{GeV})$	1.228
$C_d/(10^{-1}\,\text{GeV})$	−3.083
$D_d/(10^{-1}\,\text{GeV})$	−4.774
$E_d/\,\text{GeV}$	−2.797
$\alpha_u/^\circ$	96.64
$\beta_u/^\circ$	98.34

Observable	Global-fit value		Model best-fit
	Best-fit value	1σ range	
$\theta_{12}^q/^\circ$	13.03	12.98 → 13.07	12.988
$\theta_{13}^q/^\circ$	0.209	0.201 → 0.216	0.2085
$\theta_{23}^q/^\circ$	2.41	2.37 → 2.45	2.411
$\delta^q/^\circ$	69.21	66.12 → 72.31	68.516
$m_u/(10^{-3}\,\text{GeV})$	1.288	0.766 → 1.550	1.2889
$m_c/(10^{-1}\,\text{GeV})$	6.268	6.076 → 6.459	6.2677
$m_t/\,\text{GeV}$	171.68	170.17 → 173.18	171.684
$m_d/(10^{-3}\,\text{GeV})$	2.751	2.577 → 3.151	2.7507
$m_s/(10^{-2}\,\text{GeV})$	5.432	5.153 → 5.728	5.4328
$m_b/\,\text{GeV}$	2.854	2.827 → 2.880	2.8536
χ_q^2			0.0355

can be read from Table IV (quarks) and Table V (leptons), while the parametrization of the mass matrices is as follows

$$m_{u/d} = \begin{pmatrix} 0 & A_{u/d} & 0 \\ B_{u/d}\,e^{-i\alpha_{u/d}} & 0 & C_{u/d}\,e^{-i\alpha_{u/d}} \\ 0 & D_{u/d}\,e^{-i\beta_{u/d}} & E_{u/d}\,e^{-i\beta_{u/d}} \end{pmatrix},$$

$$m_\nu = \begin{pmatrix} 0 & a\,e^{i\phi_a} & 0 \\ a\,e^{i\phi_a} & b\,e^{i\phi_b} & c\,e^{i\phi_c} \\ 0 & c\,e^{i\phi_c} & d\,e^{i\phi_d} \end{pmatrix}. \tag{29}$$

The form of these matrices comes from the leading order EFT derived in Sec. 3. Taking for example the quark mass matrices $m_{u/d}$, which need to be diagonalized by a bi-unitary transformation,

$$m^{\rm diag} = V_L^\dagger m V_R = O^T P_L^\dagger m P_R O\,, \tag{30}$$

TABLE V. Best-fit values of the model parameters in the lepton sector are shown in the upper table. The global best-fit as well as their 1σ error [36–38] for the various observables are given in the second and third columns of the lower table. Also, the best-fit values of the various observables are listed in the last column of the lower table.

Parameter	Best fit
$a/(10^{-3}\,\mathrm{eV})$	9.933
$b/(10^{-2}\,\mathrm{eV})$	2.646
$c/(10^{-2}\,\mathrm{eV})$	2.475
$d/(10^{-2}\,\mathrm{eV})$	2.264
$\phi_a/^\circ$	29.87
$\phi_b/^\circ$	91.88
$\phi_c/^\circ$	3.03
$\phi_d/^\circ$	-109.97

Observable	Global-fit value		Model best-fit
	Best-fit value	1σ range	
$\theta^l_{12}/^\circ$	34.5	$33.5 \to 35.7$	34.85
$\theta^l_{13}/^\circ$	8.45	$8.31 \to 8.61$	8.432
$\theta^l_{23}/^\circ$	47.7	$46.0 \to 48.9$	48.11
$\delta^l/^\circ$	218	$191 \to 256$	258.8
$\alpha/^\circ$			65.27
$\beta/^\circ$			265.08
$\Delta m^2_{21}/(10^{-5}\,\mathrm{eV}^2)$	7.55	$7.39 \to 7.75$	7.571
$\Delta m^2_{32}/(10^{-3}\,\mathrm{eV}^2)$	2.424	$2.394 \to 2.454$	2.4221
$\sum m_\nu/(10^{-2}\,\mathrm{eV})$			6.453
$m_e/\,\mathrm{MeV}$	0.4865763	$0.4865735 \to 0.4865789$	-
$m_\mu/\,\mathrm{GeV}$	0.10271897	$0.10271866 \to 0.10271931$	-
$m_\tau/\,\mathrm{GeV}$	1.74618	$1.74602 \to 1.74633$	-
χ^2_l			2.0053

where, m is a quark mass matrix, $V_{L/R}$ are unitary transformation, O is an orthogonal transformation, and $P_{L/R}$ are diagonal phase matrices, for the left- and right-handed transformations, respectively. It is worth noting, that the u/d subscript has been dropped, since the procedure is the same for the up- and down-type quarks.

First, one of the six global phases can be absorbed by the fields, leaving only five phases to be redefined. This means that it is possible to write $P_L = \mathrm{diag}(1,\, e^{i\alpha},\, e^{i\beta})$, $P_R = \mathrm{diag}(e^{i\rho_1},\, e^{i\rho_2},\, e^{i\rho_3})$. It is then possible to reparametrize the fields such that $m \to P_L m P_R^\dagger$, and m^{diag} is only written in terms of real parameters. This implies that the entire complex structure of the mass matrices is entirely contained in the phase matrices. Furthermore, the number of free phases can be reduced to just two, as the CKM matrix only involves the left-handed transformations

$$\begin{aligned} V_{CKM} &= (V_L^\dagger)_u (V_L)_d = (O^T P_L^\dagger)_u (P_L O)_d \,, \\ &= O_u^T \mathrm{diag}(1,\, e^{-i(\alpha_u-\alpha_d)},\, e^{-i(\beta_u-\beta_d)}) O_d \,. \end{aligned} \quad (31)$$

In other words, it is possible to set $P_R = \mathbf{1}_3$, and since only phase differences appear in the CKM matrix, it is possible to get rid of two other phases, leaving only two phases as free parameters. In this case, the free phases are chosen to be α_u and β_u. The reduction process for the neutrinos is similar. Nevertheless, in this work it is not necessary to reduce the parameters of the neutrino mass matrix, as there are enough fitting parameters to account for the free parameters in the neutrino matrix.

4.2. Flavour violating decays with axions

Flavour violating processes containing quarks are particularly interesting, as they can have an axion in the final state [39], *i.e.*

$$q_i \to q_j a, \quad (32)$$

where the quark q_i can decay to the quark q_j and an axion. At low energies, these processes can be studied from the effective axion-quark lagrangian, and are independent of UV-completion. The parameters for the effective lagrangian are obtained from the χ^2-fit.

A particularly sensitive test of neutral flavour violation is the $K^+ \to \pi^+ a$ decay, where for this model we have

$$\Gamma(K^+ \to \pi^+ a) \approx \frac{1.9 \times 10^{-9}\text{GeV}^3}{v_\sigma^2} \ . \tag{33}$$

The E949 collaboration [40] sets the strongest constraint on this branching ratio, which is

$$\text{BR}(K^+ \to \pi^+ a) = \frac{\Gamma(K^+ \to \pi^+ a)}{\Gamma_{Total}(K^+)} < 7.3 \times 10^{-11} \ . \tag{34}$$

This translates to $v_\sigma \geqslant 2.5 \times 10^{10}\,\text{GeV}$. And from the relationship between v_σ and f_a, $v_\sigma \approx \sqrt{2} f_a N$ with $N = 5$, the bounds on v_σ can be shifted to the axion decay constant

$$f_a \geqslant 7 \times 10^9\,\text{GeV} \ . \tag{35}$$

This is the kaon decay constraint which can be seen in Fig. 3.

5. Conclusions

A DFSZ-like model was constructed, where the Peccei-Quinn and the Froggatt-Nielsen symmetries are identified. For the quark sector two UV-completions are provided. This permits generating, via the Froggatt-Nielsen mechanism, a fermion mass hierarchy, while from the same symmetry, but now via the Peccei-Quinn mechanism, allows to solve the strong CP problem. A flavourful axion arises from the theory's spectrum. The model was constructed in such a way, that the quark mass matrices have an NNI texture, where as the neutrino mass matrix has an A_2 texture.

Properties of this axion are directly obtained from the theory's parameters, as well as from a study of flavour violating decays with axions, for which the parameters for a low-energy effective theory are obtained from a χ^2 fit. This axion has the peculiarity that it is very weakly interacting, about an order of magnitude less than standard benchmark axions, and will most likely also evade future measurements. Besides this, results from the χ^2 fit also show that the NNI and A_2 textures for the quark and neutrino mass matrices, respectively, are in good agreement with current measurements and global fits.

Acknowledgments

This work is supported by the CONACyT CB-2017-2018/A1-S-13051, al Progama de Apoyo a Proyectos de Investigación e Innovación Tecnológica (PAPIIT) de la UNAM IN107118 e IN107621 grants, and the German-Mexican collaboration grant SP 778/4-1 (DFG) y 278017 (CONACyT). I thank DGAPA-UNAM for the scholarship I received. I am very grateful towards Dr. Eduardo Peinado, Dr. Newton Nath and León García for their collaboration and advice.

---

i. The strong CP problem consists on the appearance of the θ-*term*, $\theta[g_s^2/32\pi^2]G\widetilde{G}$, in the QCD lagrangian [3], itself induced by instantons and the vacuum structure of QCD. This term is C-, but not P-invariant, and therefore not CP-invariant. This term, and a contribution from the quark mass matrices provide the physical parameter $\overline{\theta} = \theta + \text{Arg}\left(\text{Det}(M^u M^d)\right)$, which has to be smaller than 10^{-10}, as it contributes to the neutron's electric dipole moment [4]. The unnatural smallness of this parameter, especially compared to weak CP violation is the strong CP problem.

ii. The axion is a massive boson, since the PQ symmetry is broken explicitly by the PQ chiral anomaly, itself induced by instantons.

iii. For a current complete review on QCD axion physics see for example [12].

iv. In this work, flavourful axion is the preferred term, since it translates nicely to Spanish as *axión sabroso*.

v. The Fritzsch texture has trouble replicating the small value of V_{cb} in the CKM matrix simultaneously with the large value of m_t [27, 28].

1. R. Peccei and H. R. Quinn, CP Conservation in the Presence of Instantons, *Phys. Rev. Lett.* **38** (1977) 1440.

2. R. D. Peccei and H. R. Quinn, Constraints Imposed by CP Conservation in the Presence of Instantons, *Phys. Rev. D* **16** (1977) 1791.

3. G. 't Hooft, Symmetry Breaking Through Bell-Jackiw Anomalies, *Phys. Rev. Lett.* **37** (1976) 8.

4. nEDM Collaboration, C. Abel et al., Measurement of the permanent electric dipole moment of the neutron, *Phys. Rev. Lett.* **124** (2020) 081803, arXiv:2001.11966 [hep-ex].

5. S. Weinberg, A New Light Boson?, *Phys. Rev. Lett.* **40** (1978) 223.

6. F. Wilczek, Problem of Strong P and T Invariance in the Presence of Instantons, *Phys. Rev. Lett.* **40** (1978) 279.

7. M. Srednicki, Axion Couplings to Matter. 1. CP Conserving Parts, *Nucl.Phys. B* **260** (1985) 689.

8. J. E. Kim, Weak Interaction Singlet and Strong CP Invariance, *Phys. Rev. Lett.* **43** (1979) 103.

9. M. A. Shifman, A. I. Vainshtein, and V. I. Zakharov, Can Confinement Ensure Natural CP Invariance of Strong Interactions?, *Nucl. Phys. B* **166** (1980) 493.

10. A. Zhitnitsky, On Possible Suppression of the Axion Hadron Interactions. (In Russian), *Sov. J. Nucl. Phys.* **31** (1980) 260.

11. M. Dine, W. Fischler, and M. Srednicki, A Simple Solution to the Strong CP Problem with a Harmless Axion, *Phys.Lett. B* **104** (1981) 199.

12. L. Di Luzio, M. Giannotti, E. Nardi, and L. Visinelli, The landscape of QCD axion models, *Phys. Rept.* **870** (2020) 1, arXiv:2003.01100 [hep-ph].

13. L. M. G. de la Vega, N. Nath, S. Nellen, and E. Peinado, Flavored axion in the UV-complete Froggatt-Nielsen models, *Eur. Phys. J. C* **81** (2021) 608, arXiv:2102.03631 [hep-ph].
14. Y. Ema, K. Hamaguchi, T. Moroi, and K. Nakayama, Flaxion: a minimal extension to solve puzzles in the standard model, *JHEP* **01** (2017) 096, arXiv:1612.05492 [hep-ph].
15. C. D. Carone and M. Merchand, T models with high quality flaxions, *Phys. Rev. D* **101** (2020) 115032, arXiv:2004.02040 [hep-ph].
16. L. Calibbi, F. Goertz, D. Redigolo, R. Ziegler, and J. Zupan, Minimal axion model from flavor, *Phys. Rev. D* **95** (2017) 095009, arXiv:1612.08040 [hep-ph].
17. F. Arias-Aragon and L. Merlo, The Minimal Flavour Violating Axion, *JHEP* **10** (2017) 168, arXiv:1709.07039 [hep-ph]. [Erratum: *JHEP* **11** (2019) 152].
18. M. Linster and R. Ziegler, A Realistic U(2) Model of Flavor, *JHEP* **08** (2018) 058, arXiv:1805.07341 [hep-ph].
19. F. Björkeroth, E. J. Chun, and S. F. King, Accidental Peccei-Quinn symmetry from discrete flavour symmetry and Pati-Salam, *Phys. Lett. B* **777** (2018) 428, arXiv:1711.05741 [hep-ph].
20. F. Björkeroth, E. J. Chun, and S. F. King, Flavourful Axion Phenomenology, *JHEP* **08** (2018) 117, arXiv:1806.00660 [hep-ph].
21. Q. Bonnefoy, E. Dudas, and S. Pokorski, Chiral Froggatt-Nielsen models, gauge anomalies and flavourful axions, *JHEP* **01** (2020) 191, arXiv:1909.05336 [hep-ph].
22. C. Froggatt and H. B. Nielsen, Hierarchy of Quark Masses, Cabibbo Angles and CP Violation, *Nucl. Phys. B* **147** (1979) 277.
23. K. Babu, TASI Lectures on Flavor Physics, in Theoretical Advanced Study Institute in Elementary Particle Physics: The Dawn of the LHC Era, pp. 49. 2010. arXiv:0910.2948 [hep-ph].
24. G. Branco, L. Lavoura, and F. Mota, Nearest Neighbor Interactions and the Physical Content of Fritzsch Mass Matrices, *Phys. Rev. D* **39** (1989) 3443.
25. H. Fritzsch, Weak Interaction Mixing in the Six - Quark Theory, *Phys. Lett. B* **73** (1978) 317.
26. H. Fritzsch, Quark Masses and Flavor Mixing, *Nucl. Phys. B* **155** (1979) 189.
27. H. Ishimori, T. Kobayashi, H. Ohki, Y. Shimizu, H. Okada, and M. Tanimoto, Non-Abelian Discrete Symmetries in Particle Physics, *Prog. Theor. Phys. Suppl.* **183** (2010) 1. arXiv:1003.3552 [hep-th].
28. H. Fritzsch, Z.-z. Xing, and Y.-L. Zhou, Non-Hermitian Perturbations to the Fritzsch Textures of Lepton and Quark Mass Matrices, *Phys. Lett. B* **697** (2011) 357. arXiv:1101.4272 [hep-ph].
29. T. Yanagida, Horizontal Symmetry and Masses of Neutrinos, *Prog. Theor. Phys*. **64** (1980) 1103.
30. J. Schechter and J. W. F. Valle, Neutrino Masses in SU(2) x U(1) Theories, *Phys. Rev. D* **22** (1980) 2227.
31. P. H. Frampton, S. L. Glashow, and D. Marfatia, Zeroes of the neutrino mass matrix, *Phys. Lett. B* **536** (2002) 79. arXiv:hep-ph/0201008.
32. D. Espriu, F. Mescia, and A. Renau, Axion-Higgs interplay in the two Higgs-doublet model, *Phys. Rev. D* **92** (2015) 095013, arXiv:1503.02953 [hep-ph].
33. G. Grilli di Cortona, E. Hardy, J. Pardo Vega, and G. Villadoro, The QCD axion, precisely, *JHEP* **01** (2016) 034, arXiv:1511.02867 [hep-ph].
34. H. Georgi and S. L. Glashow, Unity of All Elementary Particle Forces, *Phys. Rev. Lett.* **32** (1974) 438.
35. C. O'HARE, cajohare/axionlimits: Axionlimits, July, 2020. `https://doi.org/10.5281/zenodo.3932430`.
36. S. Antusch and V. Maurer, Running quark and lepton parameters at various scales, *JHEP* **11** (2013) 115, arXiv:1306.6879 [hep-ph].
37. Particle Data Group Collaboration, P. Zyla *et al*., Review of Particle Physics, *PTEP* **2020** (2020) 083C01.
38. P. de Salas, D. Forero, C. Ternes, M. Tortola, and J. Valle, Status of neutrino oscillations 2018: 3σ hint for normal mass ordering and improved CP sensitivity, *Phys.Lett. B* **782** (2018) 633. arXiv:1708.01186 [hep-ph].
39. L. Di Luzio, Flavour Violating Axions, *EPJ Web Conf.* **234** (2020) 01005, arXiv:1911.02591 [hep-ph].
40. E949, E787 Collaboration, S. Adler et al., Measurement of the K+ -¿ pi+ nu nu branching ratio, *Phys. Rev. D* **77** (2008) 052003, arXiv:0709.1000 [hep-ex].